

Diagnosis of induction motor failures using discrete wavelet transform of an auxiliary winding voltage

Yakout Khadouj Jelbaoui¹, Lamiaa El Menzhi¹, Abdallah Saad²

¹Department of Electrical and Industrial Engineering, National School of Applied Sciences (ENSA), Abdelmalek Essaadi University, Tangier, Morocco

²Department of Electrical Engineering, National Higher School of Electricity and Mechanic (ENSEM), Hassan 2 University, Casablanca, Morocco

Article Info

Article history:

Received Dec 22, 2021

Revised Jun 15, 2022

Accepted Jul 7, 2022

Keywords:

Auxiliary winding voltage

Discrete wavelet transform

Fault diagnosis

Modeling

Squirrel cage motor

ABSTRACT

Over last years, great attention has been developed to avoid the machines breakdown especially in the squirrel cage induction motor which suffer from different failures. The aim of this paper is to present a new method for the diagnosis of rotor bar breakage and end ring in induction machine fed by an inverter based on discrete wavelet transform applied on the voltage of an auxiliary winding as a new monitoring signature. The expression of the auxiliary winding voltage related to a small coil inserted between two stator phases is presented. The study is focused on the high-level signals of approximation and details coefficients. Thus, the evolution of any frequency of interest in the waveform is given in this paper. The method is validated by simulations of four broken bars and end ring cases under unloaded and loaded machine.

This is an open access article under the [CC BY-SA](https://creativecommons.org/licenses/by-sa/4.0/) license.



Corresponding Author:

Yakout Khadouj Jelbaoui

Department of Electrical and Industrial Engineering, National School of Applied Sciences

Abdelmalek Essaâdi University

Tangier 90000, Morocco

Email: jelbaoui.yakout@gmail.com

1. INTRODUCTION

The squirrel cage induction machine is widely used in industrial applications, it represents more than 70% of the electrical machines due to its reliability and its low maintenance costs. However, this kind of machine is often subject to several constrains during its operation and it may suffer serious damage leading to its deterioration and fail. The production shutdowns are costly in terms of time lost, maintenance costs and can cause damage to other devises. Improving the electromechanical systems operation have attracted several researchers in order to avoid downtime of the machines and guarantee its overall performance. For that reason, the preventive maintenance is important. It is based on online monitoring and diagnosis of real-time signals. Multiple methods are used to investigate diagnosis process according to various faults occurring in the machine such as bearing faults, eccentricity, broken rotor bars and stator winding inter turn faults [1]. Condition monitoring and faults diagnostics using signal analysis are the most powerful methods to detect the machine failures at the initial stage without affecting the signal contain [2], [3]. The most classical one is the fast fourier transform (FFT) that is widely used for the detection of broken rotor bars in induction machine by transforming the signal from time domain to frequency domain. This approach gives satisfactory results if the signal monitored is stationary and the machine operates under steady state mode. However, the frequencies related to the presence of broken rotor bar fault can be detected by other causes such as bearing faults and voltage fluctuations [4]. Furthermore, the stationarity of the signal changes according to the stresses and the

environment that the machine is exposed to. In this case, the FFT cannot extract the inherent information of the non-stationary signals, the fundamental frequency can mask the small characteristic frequencies produced by broken bar faults making them undistinguishable. The time frequency analysis is required to overcome the FFT disadvantages such as the short-time fourier transform (STFT) [5] which performs temporal location of different frequency components of the signal. The resolution of this method uses a constant window size for all frequencies. To adjust the time widths to the frequency the wavelet transform (WT) is used [6]-[8]. A comparative study conducted by Kim et al. proves its effectiveness [9]. Thus, the transient component will be localized to extract the components associated to the failure evolution. The wavelet which is a small wave, has time-widths that automatically change with their frequencies. It provides simultaneously time and frequency information. The WT is a powerful diagnostic technique in power applications. Many research papers have been published in this field [10]-[16]. It uses multi-resolution technique depending on the different frequencies given by the signal that means for high frequencies, the wavelet uses a low time resolution whereas a high time resolution is reached for low frequencies. In general, the wavelet transform can be categorized in two forms: continuous wavelet transform (CWT) and discrete wavelet transform (DWT) used to extract the fast transition characterizing the failures of the signal after decomposition.

In fact, in a wide range of industrial application, induction motors are used with variable speed. For this reason, the present article establishes the detection of broken rotor bars and end rings of a squirrel cage induction motor fed by an inverter [17]. Due to the inaccessibility of direct measurements of rotor parameters in asynchronous motors, a new methodology for online fault detection is presented. It is based on monitoring a novel signal related to an auxiliary winding inserted inside the machine. It's a small coil between two stator phases. The novelty of this article is to diagnose and monitor the auxiliary winding voltage through the analysis of discrete wavelet transform coefficients with a high-order mother wavelet.

2. DISCRET WAVELET TRANSFORM

The discrete wavelet transform is one of the most powerful diagnosis techniques for analyzing time frequency representation of a signal by decomposing it in a set of sub-signals [18]-[20]. It is suitable for highlight the change occurs in the signal in early stage. This technique uses a multi-resolution in order to analyze the signal through different frequency band. According to Mallat algorithm [18], [21], each signal is associated with certain frequency band. The DWT leads to a signal decomposition into multiple small wave signals. The number of this decomposition is called levels (n). The decomposition is implemented using two filters: a low pass filter, denoted as $h(k)$, containing low frequency component of the signal that determine approximation coefficient a_j ; and a high pass filter denoted as $g(k)$ containing high frequency component that identifies the detail coefficient d_j . The sum of approximation coefficients and detail can reconstruct and approximate the signal as shown in (1).

$$s(t) = \sum_i \alpha_i^n \phi_i^n(t) + \sum_{j=1}^n \sum_i \beta_i^j \psi_i^j(t) = a_n + d_n + \dots + d_1 \quad (1)$$

Where n is the decomposition level, α_i^n is the scaling coefficients and β_i^j is the wavelet coefficients, $\phi_i^n(t), \psi_i^j(t)$ are the scaling function at level n and wavelet function at level j respectively [22]. The frequency bands related to the detail coefficient d_j and approximation coefficient a_j are expressed as (2) and (3).

$$f_{d_j} \in \left[\left(\frac{f_s}{2^{(j+1)}} \right), \left(\frac{f_s}{2^j} \right) \right] \quad (2)$$

$$f_{a_j} \in \left[0, \left(\frac{f_s}{2^{(j+1)}} \right) \right] \quad (3)$$

For the application of the discrete wavelet transform the selection of the mother wavelet and the determination of the number of decomposition levels are important [23]. Recently, several mother wavelets families exist with different proprieties categorized in two kinds of wavelet. The first one is the wavelet with infinite support such as Morlet, Gaussian, Meyer, Haar, and Mexican Hat. The second one is the compact supported wavelet which is divided into biorthogonal wavelet and orthogonal wavelet such as Daubechies or Coiflet. For this kind, a high-order mother wavelet is recommended for the extraction of the small frequencies and the reconstruction of the signal without losing information. The mother wavelet function generated by a translation (a) and a scale parameter (b) is defined as (4).

$$\psi_{(a,b)}(t) = \frac{1}{\sqrt{b}}\psi\left(\frac{t-a}{b}\right) \tag{4}$$

For the feature extraction, the used dyadic scales is discretized as $a= 2^j$ where j denotes the level and $b=2$. After that, the scalar product of this mother wavelet and a function $f(t)$, gives the expression of the discrete wavelet function as (5).

$$dwt(a, b) = \langle f, \psi_{(a,b)} \rangle = \sum_{m=0}^q f(t_m) \frac{1}{\sqrt{b}}\psi\left(\frac{t_m-a}{b}\right) dt \tag{5}$$

The filters used in the DWT are constructed from the selected mother wavelet (t) and the scaling function $\phi(t)$ as (6).

$$\begin{cases} \psi(t) = \sqrt{2} \sum_k g(k)\phi(2t - k) \\ \phi(t) = \sqrt{2} \sum_k h(k)\phi(2t - k) \end{cases} \tag{6}$$

With $\sum_k g(k) = 0$ and $\sum_k h(k) = \sqrt{2}$. Therefore, the approximation and the detail coefficients corresponding to the low and high frequency components respectively are presented as (7).

$$\begin{cases} a_{j,k} = \sum_m h(2k - m)a_{j-1,k} \\ d_{j,k} = \sum_m g(2k - m) d_{j-1,k} \end{cases} \tag{7}$$

For the best failures extraction, the number of decomposition levels depends on the sampling frequency. It can be determined by the follow (8).

$$n = integer \left[\frac{\log(f_s/f)}{\log(2)} \right] \tag{8}$$

In this paper, Debauchies mother wavelet has been used for the DWT analysis in order to avoid overlapping between adjacent wavelet signals. The higher order Debauchies (dbN) gives an ideal failures extraction by using high number of filters, for db40, the filter length corresponding is $L_{db40} = 2N = 80$. The fundamental frequency is $f_s = 50 Hz$, the sampling frequency is $f_s = 10,000$ samples/s, the application of (6) leads to $n = 7$. According to (2) and (3) the frequency bands associated to each level is presented in Table 1. When the number of decomposition levels increase, the frequency bands of DWT correspondent decrease. The detail d_1 includes the high frequency component of the signal and the low frequencies includes in a_7 .

Table 1. Frequency bands for the Wavelet signals

Levels	Approximation signals a_j (Hz)		Detail signals d_j (Hz)	
j=1	a_1	0-2500	d_1	2500-5000
j=2	a_2	0-1250	d_2	1250-2500
j=3	a_3	0-625	d_3	625-1250
j=4	a_4	0-312.5	d_4	312.5-625
j=5	a_5	0-156.25	d_5	156.25-312.5
j=6	a_6	0-78.125	d_6	78.125-156.25
j=7	a_7	0-39.0625	d_7	39.0625-78.125

3. AUXILIARY WINDING VOLTAGE

The aim of the proposed method consists of inserting a small coil as a “sneak” between two stator phases. The technic is built considering the auxiliary winding that forms an angle θ_0 with the A stator phase as shown in Figure 1. Therefore, the inserted coil has no conductive contact with the other phases. It is coupled mutually with all the motor circuits in the stator and the rotor. The determination of the auxiliary winding voltage is the main key of this approach. Monitoring this signal is extremely beneficial to achieve an efficient diagnosis of the squirrel cage induction machine [24], [25]. This technic was applied previously for a wound rotor induction machine [26], [27]. The mathematical model of the squirrel cage induction machine fed by an inverter is presented in [17].

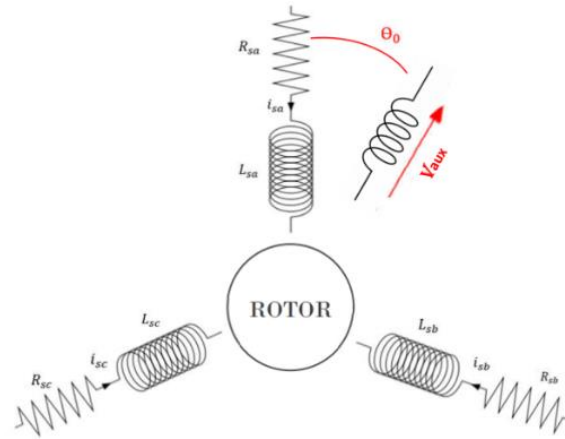


Figure 1. Auxiliary winding emplacement inside the squirrel cage induction motor

The mathematical model of this method is presented in this section. As known, the voltage is a derivation of the flux. Therefore, the auxiliary winding voltage is expressed as (9).

$$V_{aux} = \frac{d \varphi_{aux}}{dt} \tag{9}$$

From the current vector $I = [I_{sa}, I_{sb}, I_{sc}, I_{r1}, \dots, I_{ri}, \dots, I_{rn}]$ obtained from the squirrel cage induction machine fed by an inverter, the auxiliary winding flux is defined as (10).

$$\varphi_{aux} = a I_{sa} + b I_{sb} + c I_{sc} + \sum_{i=1}^{Nr} d_j I_{ri} \tag{10}$$

The coefficients a, b, c and d_j depend on the angle θ_0 , as shown in [13],

$$a = M_{saux} \cos(\theta_0), \quad b = M_{saux} \cos\left(\frac{2\pi}{3} - \theta_0\right), \quad c = M_{saux} \cos\left(\frac{4\pi}{3} - \theta_0\right), \quad d_j = M_{raux} \cos\left(\theta + \frac{j\pi}{3}\right), \quad j = 0, 2, 4 \dots$$

M_{saux}, M_{raux} are the mutual inductances of the inserted coil with the stator phases and the rotor bars respectively. In order to form a three-phase system with the auxiliary winding, we consider two other fictive coils. Their shift phase angles are 120° . The expressions of the voltage in these fictive coils are (11).

$$V_{auxa} = \frac{d \varphi_{auxa}}{dt}, \quad V_{auxb} = \frac{d \varphi_{auxb}}{dt}, \quad V_{auxc} = \frac{d \varphi_{auxc}}{dt} \tag{11}$$

After testing different value of θ_0 , this angle does not affect the simulation results. Therefore, we choose $\theta_0=0$. Thus, the auxiliary winding flux of the phase A is represented as (12) and (13).

$$\varphi_{auxa} = \varphi_{sa} + \varphi_{sb} + \varphi_{sc} + \sum_{i=1}^{Nr} \varphi_{ri} \tag{12}$$

$$\varphi_{auxa} = M_{saux} I_{sa} - \frac{M_{saux}}{2} I_{sb} - \frac{M_{saux}}{2} I_{sc} + \sum_{i=1}^{Nr} M_{raux} \cos\left(\theta + \frac{j\pi}{3}\right) I_{ri}, \quad j = 0, 2, 4 \dots \tag{13}$$

4. SIMULATION RESULT AND DISCUSSIONS

In this section, the proposed method is applied to diagnose a 450W squirrel cage induction machine fed by an inverter under several faults and operation conditions. The simulation is carried out by MATLAB wavelet toolbox for performing DWT of the auxiliary winding voltage signal with seven levels corresponding to different frequency bands as shown in table 1; whereas Daubechies-40 was selected as the mother wavelet. The performance of the proposed method for fault detection is tested in different rotor bar breakages cases and under load levels. The characteristic of the simulated motor is presented in Table 2.

The motor fed by an inverter has been tested under five cases with 2 load conditions: healthy state, the presence of a broken bar, two broken bars, five broken bars and two broken bars with one broken end ring. The supply frequency f is included in details d_7 . The frequencies below f are included in the

approximation of the level 7 a_7 . The higher-level signals associated to the frequency bands below the supply frequency, are discussed in this section. The results show the advantage of the time-frequency representation of the signal. The oscillations occur in different frequency bands at the same time as shown in Figure 2. Figure 2(a) and Figure(b) present the sampled auxiliary winding voltage signal (s at the top) and the signals resulting from the DWT for the healthy state in the case of an unloaded machine and in the case of a motor with $Cr=3Nm$. The detail d_6 reproduces the analyzed auxiliary winding voltage. The signals a_7 , d_7 and d_6 do not present any variation. The non-defected machine case is considered as a reference for this study to which the faulty cases will be compared.

Table 2. Motor Specifications

Symbol	quantity	Value
V	Power supply voltage	220/380 V
f	Frequency	50 Hz
p	Number of poles pairs	1
N_r	Number of rotor bars	27
N_s	Number of stator slots	193
R_s	Resistance of stator winding	4.1 Ω
R_b	Resistance of a rotor bar	74 $\mu\Omega$
R_e	Resistance of the rotor end ring	74 $\mu\Omega$
L_b	Leakage inductance of rotor bars	0.33 μH
L_e	Leakage inductance of rotor end rings	0.33 μH
J	Moment of inertia	4.5 10^{-3} Nms ²

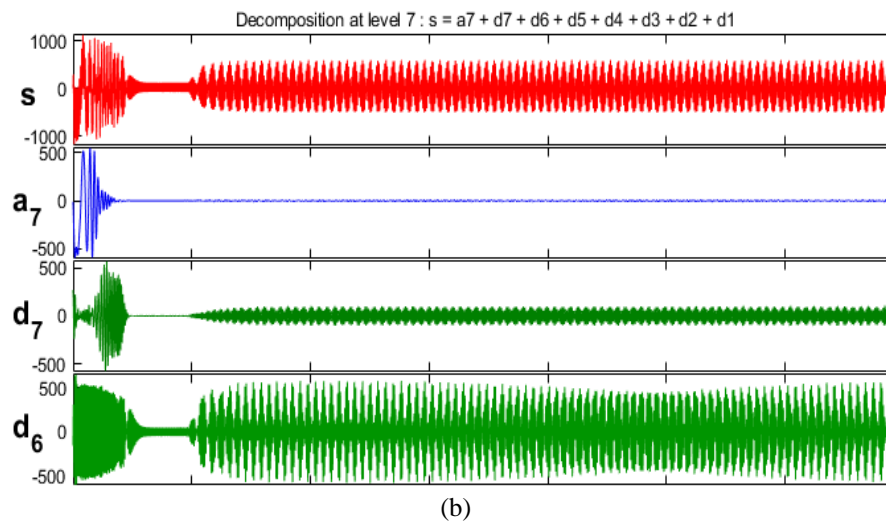
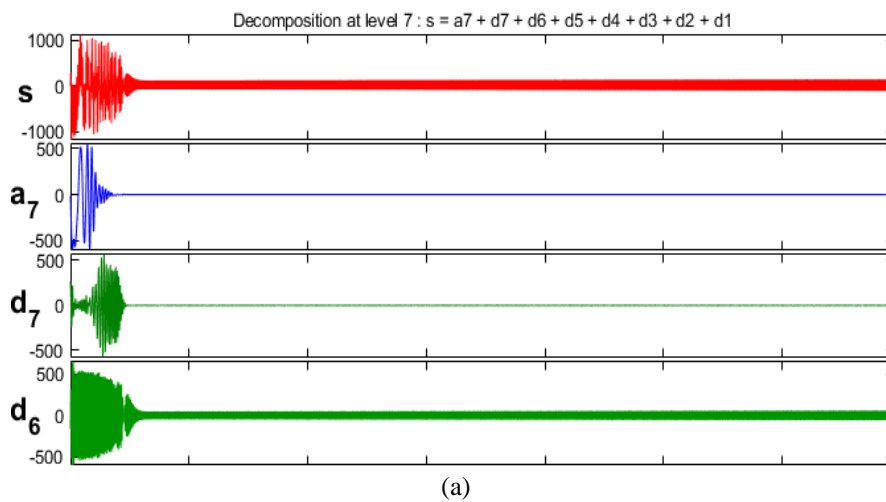


Figure 2. Wavelet analyses of auxiliary winding voltage for healthy state in case of (a) unloaded machine and (b) $Cr=3 Nm$

For the breakage of one rotor bar presented in Figure 3, in the case of an unloaded machine, in Figure 3(a) a small variation appears at $t=1.97$ s. The oscillation amplitude in the approximation signal a_7 is 4.46 V. In the details d_7 , it corresponds to 25.33 V. When the load increases to $Cr=3$ Nm as shown in Figure 3(b), the oscillation amplitude increases to 25.27 V and to 151V for the approximation a_7 and the detail d_7 respectively.

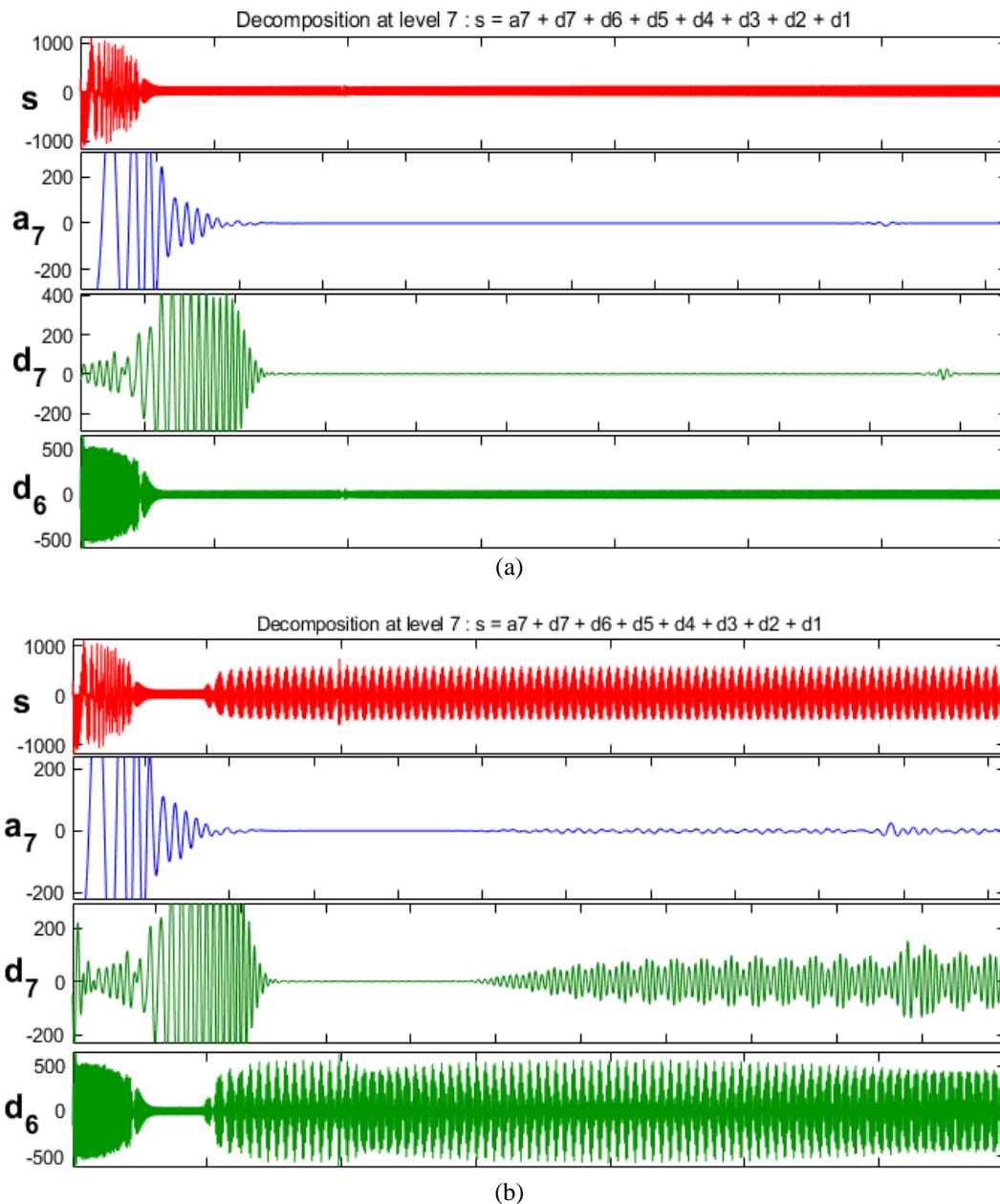


Figure 3. Wavelet analyses of auxiliary winding voltage for one broken bar in case of (a) unloaded machine and (b) $Cr=3$ Nm

Figure 4 present the case of two broken bars, in Figure 4(a) more oscillations appear in the approximation signal a_7 . The first one occurs at $t=1.97$ s with an amplitude of 4.445 V. The other one occurs at $t=2.573$ s with an amplitude of 6.581 V. The details signal d_7 shows two oscillations at $t=1.97$ s corresponding to an amplitude of 25.33 V and a large oscillation at $t=2.564$ s with an amplitude of 74.79 V. When the load level reaches $Cr=3$ Nm, as shown in Figure 4(b), for the approximation signal a_7 , the

oscillations amplitudes increase to 23.93 V and 27.22 V at the same time as the previous case. The details signal d_7 reaches 152.4 V and 172.5V respectively at $t=1.97$ s and $t=2.564$ s.

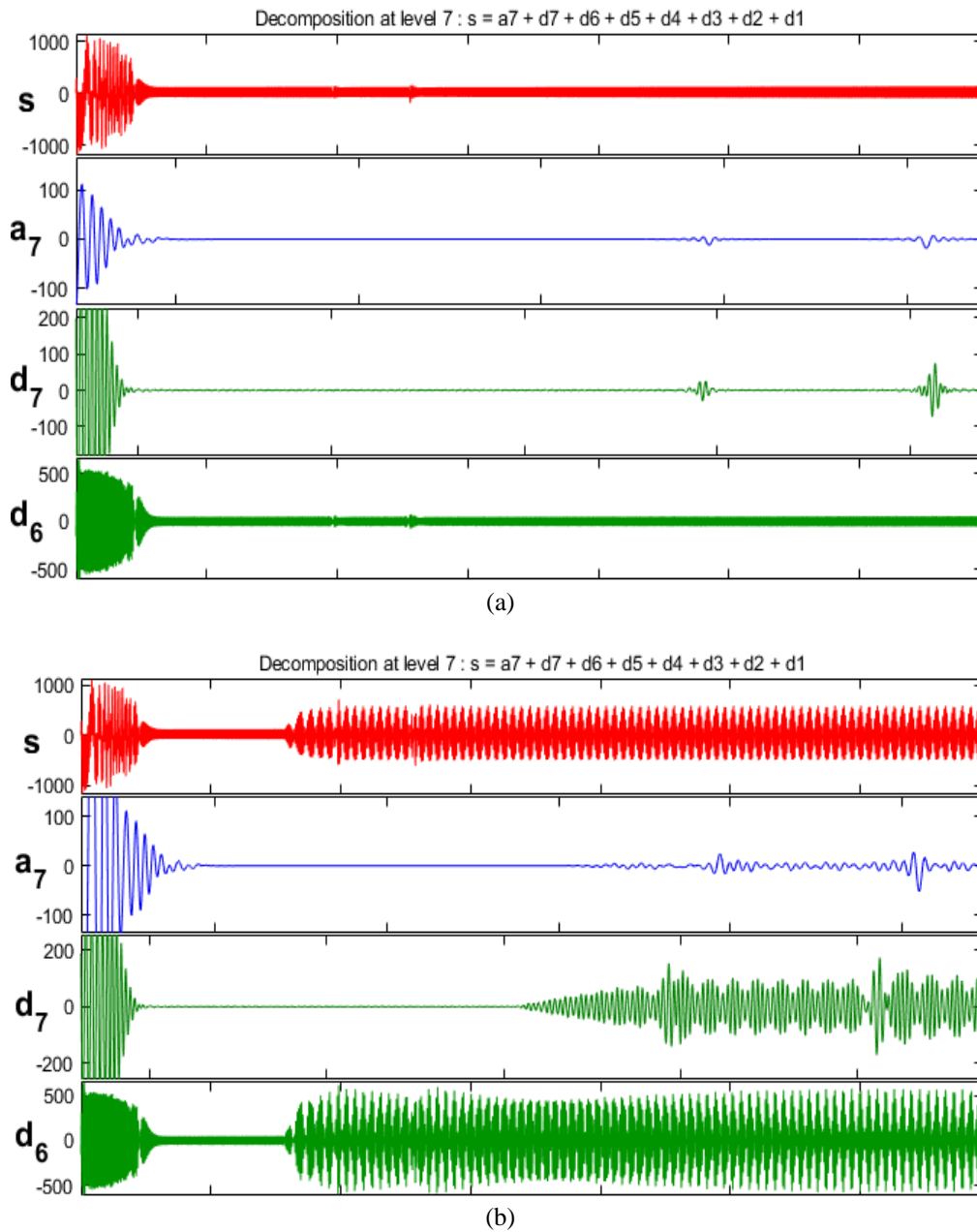


Figure 4. Wavelet analyses of auxiliary winding voltage for two broken bars in case of (a) unloaded machine and (b) $Cr=3$ Nm

Multiple oscillations with different width shown in Figure 5 are produced by five broken bars. In the case of an unloaded machine in Figure 5(a), the oscillations appear at a_7 from $t=1.54$ s with an amplitude of 4.451 V until $t=3.5$ s that corresponds to the amplitude of 47.96 V. The detail d_7 presents the same variation and has different amplitudes and width starting from $t=1.558$ s with 21.76 V until $t=3.55$ s corresponding to an amplitude of 121.6 V. At $t=2.96$ s, an oscillation amplitude attends 136.8 V. In the case of $Cr=3$ Nm presented in Figure 5(b), a clear perturbation appears with the evolution of a_7 over the time. From $t=1.572$ s to $t=3.559$ s, the oscillations present an amplitude of 29.31 V and 27.8 V respectively. The maximum amplitude reaches 61.02 V at $t=2.96$ s. Moreover, d_7 shows the largest variation at $t=3.1$ s with an amplitude

of 421.5 V. Other one starts from $t=1.57$ s to $t=3.536$ s. Their amplitudes are 127.7 V and 190.8 V respectively.

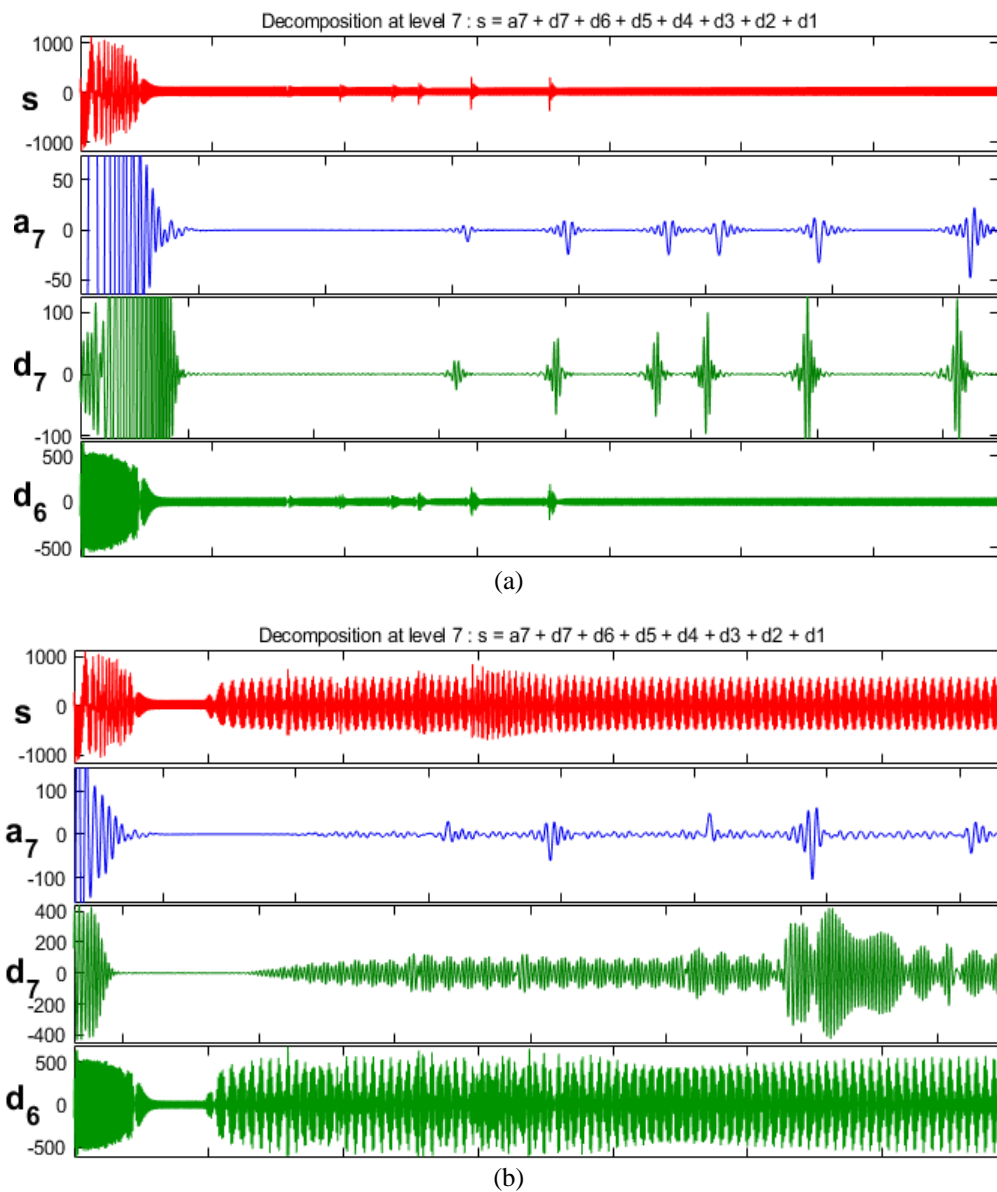


Figure 5. Wavelet analyses of auxiliary winding voltage for five broken bars in case of (a) unloaded machine and (b) $Cr=3$ Nm

The breakage of two adjacent bars causes the breakage of an end ring. In this case, Figure 6 shows the variation that occurs in the auxiliary winding voltage within the approximation and the details signals. For an unloaded machine in Figure 6(a), three oscillations in a_7 with different width and amplitude as 4.445 V, 6.581 V and 6.142 V appear at $t=1.943$ s, $t=2.573$ s and $t=2.93$ s respectively. The oscillations presented in the detail d_7 occur at $t=1.955$ s with an amplitude of 23.84 V until $t=2.961$ s that corresponds to an amplitude of 74.56 V. For $Cr=3$ Nm Figure 6(b), the oscillations amplitude increase. The signal a_7 present three oscillations with an amplitude around 25 V. The signal d_7 shows larger oscillations with an amplitude that reaches 162 V at $t=2.186$ s.

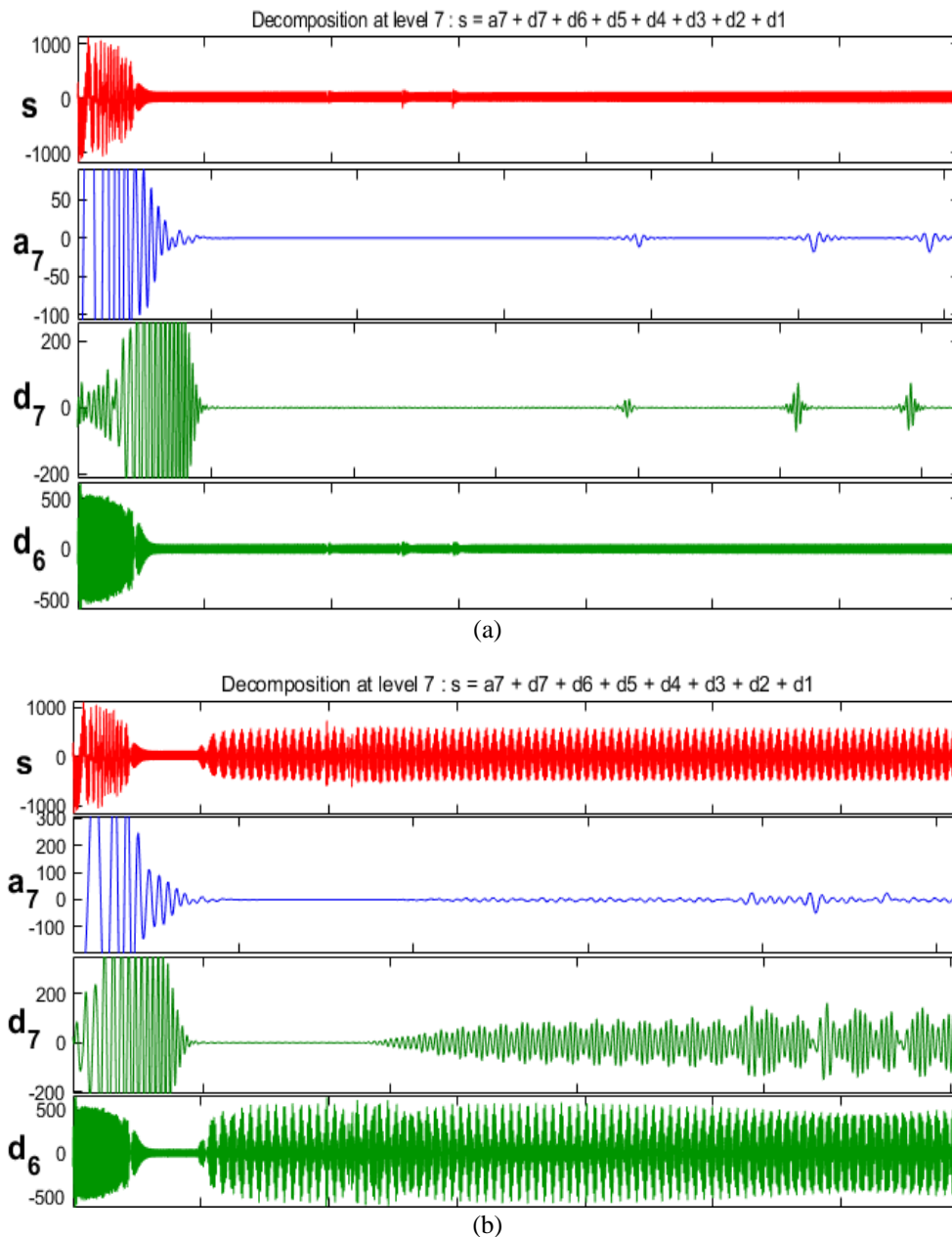


Figure 6. Wavelet analyses of auxiliary winding voltage for two broken bars with one broken end ring in case of (a) unloaded machine and (b) $C_r=3$ Nm

5. CONCLUSION





This paper has introduced a new method to diagnose rotor broken bar and end rings fault in induction motor fed by an inverter. The method is based on the application of discrete wavelet transform to the auxiliary winding voltage of an inserted coil between two phases in the machine stator side. The method is tested on MATLAB software under different faulty conditions. The simulation results show the effectiveness of this approach to provide a time-frequency localization and prove the ability of the proposed signal for the failures extraction even in the case of an unloaded condition.

REFERENCES





- [1] X. Liang and K. Edomwandekhoe, "Condition monitoring techniques for induction motors," in *2017 IEEE Industry Applications Society Annual Meeting*, 2017, pp. 1-10, doi: 10.1109/IAS.2017.8101860.
- [2] S. A. Taher and M. Malekpour, "A novel technique for rotor bar failure detection in single-cage induction motor using FEM and MATLAB/SIMULINK," *Mathematical Problems in Engineering*, vol. 2011, p. 620689, 2011, doi: 10.1155/2011/620689.

- [3] K. M. B. Gamal, S. Handa, and M. R. Murthy, "A fault diagnostic method for monitoring induction motor," *International Journal of Engineering Science and Computing*, vol. 7, no. 2, pp. 4610-4615, 2017.
- [4] M. F. Cabanas, M. G. Melero, and G. A. Capolino, "A new methodology for applying the FFT to induction machine on-line diagnosis," in *Proceedings IEEE- Symposium on Diagnostics for Electrical Machines, Power Electronics and Drives (SDEMPED) 1999*, 1999, pp. 537-543.
- [5] I. S. Koo and W. W. Kim, "Development of reactor coolant pump vibration monitoring and a diagnostic system in the nuclear power plant," *ISA Transactions*, vol. 39, no. 3, 2000, pp. 309-316, doi: 10.1016/s0019-0578(00)00019-7.
- [6] H. Douglas, P. Pillay, and A. K. Ziarani, "A new algorithm for transient motor current signature analysis using wavelets," *IEEE Transactions on Industry Applications*, vol. 40, no. 5, pp. 1361-1368, Sept.-Oct. 2004, doi: 10.1109/TIA.2004.834130.
- [7] L. Daubechies, "The wavelet transform, time-frequency localization and signal analysis," *IEEE Transactions on Information Theory*, vol. 36, no. 5, pp. 961-1005, Sep. 1990, doi: 10.1109/18.57199.
- [8] Z. Zhang and Z. Ren, "A novel detection method of motor broken rotor bars based on wavelet ridge," *IEEE Transactions on Energy Conversion*, vol. 18, no. 3, pp. 417-423, Sept. 2003, doi: 10.1109/TEC.2003.815851.
- [9] B. Kim, S. Lee, M. Lee, J. Ni, J. Yeob. Song, C. Lee, "A comparative study on damage detection in speed-up and coast-down process of grinding spindle-typed rotor-bearing system," *Journal of Materials Processing Technology*, vol. 187, pp. 30-36, 2007, doi: 10.1016/j.jmatprotec.2006.11.222.
- [10] A. W. Galli, G. T. Heydt, and P. F. Riberio, "Exploring the power of wavelet analysis," *IEEE Computer Applications in Power*, vol. 9, no. 4, pp. 37-41, Oct. 1996, doi: 10.1109/67.539845.
- [11] P. Pillay, P. Ribeiro, and Q. Pan, "Power quality modeling using wavelets," in *IEEE Proceedings of the 7th International Conference on Harmonics and Quality of Power (ICHQP)*, pp. 625-631, Oct. 1996.
- [12] A. M. Gaouda, S. H. Kanoun, M. M. A. Salama, and A. Y. Chikhani, "Wavelet-based signal processing for disturbance classification and measurement," *IEE Proceedings - Generation, Transmission and Distribution*, vol. 149, no. 3, pp. 310-318, 2002, doi: 10.1049/ip-gtd:20020119.
- [13] K. Siddiqui, V. K. Giri, "Broken rotor bar fault detection in induction motors using wavelet transform," *2012 International Conference on Computing, Electronics and Electrical Technologies (ICCEET)*, 2012, pp. 1-6, doi: 10.1109/ICCEET.2012.6203753.
- [14] C. H. Lee, "Wavelet based transient analysis," Ph.D. dissertation, School of Electrical and Computer Engineering, Georgia Institute of Technology, Georgia, 1998.
- [15] F. Ponci, A. Monti, L. Cristaldi, and M. Lazzaroni, "Diagnostic of a faulty induction motor drive via wavelet decomposition," *IEEE Transactions on Instrumentation and Measurement*, vol. 56, no. 6, pp. 2606-2615, Dec. 2007, doi: 10.1109/TIM.2007.907943.
- [16] M. Aktas and V. Turkmenoglu, "Wavelet-based switching faults detection in direct torque control induction motor drives," *IET Science, Measurement & Technology*, vol. 4, no. 6, pp. 303-310, 2010, doi: 10.1049/iet-smt.2009.0121.
- [17] Y. K. Jelbaoui, E. M. Lamiaa, and A. Saad, "Fault diagnosis of a squirrel cage induction motor fed by an inverter using lissajous curve of an auxiliary winding voltage," *Indonesian Journal of Electrical Engineering and Computer Science*, vol. 21, no. 3, pp. 1299-1308, 2021, doi: 10.11591/ijeecs.v21.i3.pp1299-1308.
- [18] M. Stéphane, *A wavelet tour of signal processing*, New York: Academic Press, 2008.
- [19] M. Riera-Guasp, J. A. Antonino-Daviu, M. Pineda-Sanchez, R. PuchePanadero, and J. Perez-Cruz, "A general approach for the transient detection of slip-dependent fault components based on the discrete wavelet transform," *IEEE Transactions on Industrial Electronics*, vol. 55, no. 12, pp. 4167-4180, Dec. 2008, doi: 10.1109/TIE.2008.2004378.
- [20] W. G. Zanardelli, E. G. Strangas, H. K. Khalil, and J. M. Miller, "Wavelet-based methods for the prognosis of mechanical and electrical failures in electric motors," *Mechanical Systems and Signal Processing*, vol. 19, no. 2, pp. 411-426, 2005, doi: 10.1016/j.ymssp.2003.10.002.
- [21] Stephane G. Mallat, "A Theory for Multiresolution Signal Decomposition: The Wavelet Representation," *IEEE Transactions on Pattern Analysis and Machine Intelligence*, vol. 11, no. 7, pp. 674-693, Jul. 1989, doi: 10.1109/34.192463.
- [22] J. A. Antonino-Daviu, M. Riera-Guasp, J. R. Folch and M. P. M. Palomares, "Validation of a new method for the diagnosis of rotor bar failures via wavelet transform in industrial induction machines," in *IEEE Transactions on Industry Applications*, vol. 42, no. 4, pp. 990-996, July-Aug. 2006, doi: 10.1109/TIA.2006.876082.
- [23] C. S. Burrus, R. A. Gopinath, and H. Guo, *Introduction to wavelets and wavelet transforms: a primer*, Englewood Cliffs, New Jersey: Prentice Hall, 1998.
- [24] Y. K. Jelbaoui, E. M. Lamiaa, and A. Saad, "Squirrel cage induction motor fault diagnosis using lissajous curve of an auxiliary winding voltage: case of broken bars," *Indonesian Journal of Electrical Engineering and Computer Science*, vol. 24, no. 3, pp. 1332-1341, 2021, doi: 10.11591/ijeecs.v24.i3.pp1332-1341.
- [25] Y. K. Jelbaoui, E. M. Lamiaa, and A. Saad, "Diagnosis of rotor faults by fast Fourier transform using an auxiliary winding voltage," *Indonesian Journal of Electrical Engineering and Computer Science*, vol. 24, no. 2, pp. 680-688, 2021, 10.11591/ijeecs.v24.i2.pp680-688.
- [26] L. El Menzhi and A. Saad, "Three phase induction motor inverter defects diagnosis using voltage spectrum of an auxiliary winding," *Applied Mechanics and Materials*, vol. 672-674, pp. 1244-1252, 2014, doi: 10.4028/www.scientific.net/AMM.672-674.1244.
- [27] L. El Menzhi and A. Saad, "Lissajous curve of an auxiliary winding voltage park components for diagnosing multiple open switches faults in three phase inverter," *Applied Mechanics and Materials*, vol. 672-674, pp. 1224-1233, 2014, doi: 10.4028/www.scientific.net/AMM.672-674.1224.





BIOGRAPHIES OF AUTHORS

Yakout Khadouj Jelbaoui     was born in Morocco on July 1992. In 2015, she received the Engineer degree in Mechatronics from the National School of Applied Sciences, Abdelmalek Essaadi University of Morocco in Tetouan. She is PhD student in Electrotechnical engineering at National School of Applied Sciences in Tangier since November 2016. She is interested in electrical machines and electrical devices modeling, control and on-line diagnosis defects. She can be contacted at email: jelbaoui.yakout@gmail.com.



Prof. Dr. Lamiaa El Menzhi     is a professor in Abdelmalek Essaadi University in Morocco since 2010. On 2002, She got her High Deepened Studies Diploma in electrical engineering from the High National School of Electricity and Mechanics ENSEM in Hassan 2 University in Casablanca. From 2002 until 2004, she was a research student in one of the universities in japan. On 2009, she obtained her Doctor degree, then her Habilitation as a professor researcher on 2016 from Hassan 2 University in Casablanca (ESEM). She is interested in electrical machines control and on-line diagnosis either used as a motor or a generator in wind turbines. Lamiaa El Menzhi is a member and advisor of the Moroccan Center of Polytechnical Research and Innovation since 2015. She can be contacted at email: lamdockit@yahoo.com.



Prof. Dr. Abdallah Saad     was born in Morocco in September 1956. He received the Engineer and Doctor of Engineering degrees from National Polytechnic Institute of Grenoble France respectively in 1980 and 1982. From 1982 to 1986, he was Researcher at French National Center for Scientific Research (CNRS)-Electrostatics and Dielectric Materials Laboratory Grenoble. After receiving the Doctor of Physical Sciences degree in 1986, he joined Hassan 2 University of Morocco. Professor of electrical engineering, he has several scientific and educational responsibilities. His main fields of interest are High Voltage and Electrical Insulations, modeling and control, renewable energy integration. He can be contacted at email: saad.abdal@gmail.com.